

# Exploring Optimal Latent Trajectory for Zero-shot Image Editing

Maomao Li<sup>1,2</sup>, Yu Li<sup>2\*</sup>, Yunfei Liu<sup>2</sup>, Dong Xu<sup>1\*</sup>

<sup>1</sup>School of Computing and Data Science, The University of Hong Kong

<sup>2</sup>International Digital Economy Academy (IDEA)

limaomao07@connect.hku.hk {liyu, liuyunfei}@idea.edu.cn dongxu@hku.hk

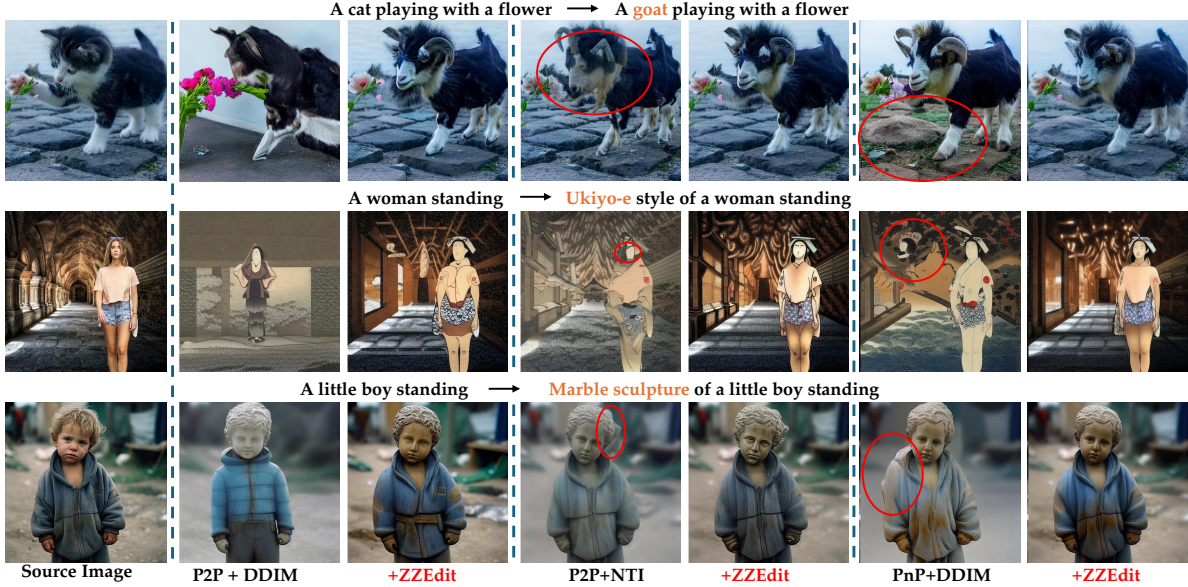


Figure 1. We propose a new editing paradigm dubbed ZZEdit, which demonstrates a more subtle editability and fidelity over the commonly employed “inversion-then-editing” pipeline. Moreover, it seamlessly integrates with contemporary text-driven image editing methods, such as P2P [15] (with DDIM inversion [40] or Null-text inversion [26]) and PnP [43] (with DDIM inversion), enhancing their capabilities. Without training or finetuning, our ZZEdit shows the feasibility of using dynamic latent trajectory on the existing image editing techniques.

## Abstract

*Editability and fidelity are two essential demands for text-driven image editing, which expects that the editing area should align with the target prompt and the rest should remain unchanged separately. The current cutting-edge editing methods usually obey an “inversion-then-editing” pipeline, where the source image is first inverted to an approximate Gaussian noise  $z_T$ , based on which a sampling process is conducted using the target prompt. Nevertheless, we argue that it is not a good choice to use a near-Gaussian noise as a pivot for further editing since it almost lost all structure fidelity. We verify this by a pilot experiment, discovering that some intermediate-inverted latents can achieve a better trade-off between editability and fidelity than the fully-inverted  $z_T$ . Based on this, we propose a novel editing paradigm dubbed ZZEdit, which gently*

*strengthens the target guidance on a sufficient-for-editing while structure-preserving latent. Specifically, we locate such an editing pivot by searching the first point on the inversion trajectory which has larger response levels toward the target prompt than the source one. Then, we propose a ZigZag process to perform mild target guiding on this pivot, which fulfills denoising and inversion iteratively, approaching the target while still holding fidelity. Afterwards, to achieve the same number of inversion and denoising steps, we perform a pure sampling process under the target prompt. Extensive experiments highlight the effectiveness of our ZZEdit in diverse image editing scenarios compared with the “inversion-then-editing” pipeline.*

## 1. Introduction

Recent years, large-scale text-guided diffusion models [14, 33, 35, 38, 48] have attracted growing attention in com-

\*Corresponding Author

puter vision and graphics community, showing efficiency for high-quality text-to-image (T2I) synthesis. To replicate this success into text-guided image editing and enable users to manipulate input images according to their text prompt, early attempts usually take additional user-provided masks [3, 11, 25, 27, 34] or box [23]. Besides, [31, 50] take more conditions for fine-grained control over images e.g., depth maps, canny edges, poses, and sketches. Another line of research aims for *text-only* interactive image editing [4, 6, 9, 15, 19, 24, 26, 43]. Since the last setting operates with minimal input conditions (i.e., only image and text) but also shows promising results for real image editing, we follow their trend in this work.

The current text-only image editing methods usually obey the “inversion-then-editing” pipeline. Specifically, inversion techniques gradually add noise to the source image feature  $z_0$  until reaching an approximate Gaussian noise  $z_T$ , based on which a sampling process is carried out under the guidance of the target-prompt. Here, we raise a question that *is it a good choice to directly invert the input image to a near-Gaussian noise?* We believe the answer is negative from the perspective of both *editability* and *fidelity*. For the former, as seen in Fig. 2, we conduct a pilot experiment with commonly-used DDIM inversion, and discover that there are a lot of intermediate-inverted latents that can provide considerable or greater editability than  $z_T$ . For the latter, given that DDIM inversion has accumulated errors in each step [9, 19, 26], applying  $z_T$  for subsequent denoising would inevitably bring more reconstruction errors than intermediate-inverted ones, thus hindering the fidelity.

In view of the above considerations, we attempt to use an intermediate-inverted latent which has sufficient editability while still keeping certain structure information as the editing pivot. To this end, we propose a novel editing paradigm, dubbed ZZEdit, where the insight behind is *mildly strengthening guidance at a structure-preserving while sufficient-for-editing point*. Specifically, starting from  $z_0$ , we locate the qualified editing pivot by looking up the *first* step on the inversion trajectory whose response to the target prompt is greater than that to the source one. Then, we propose a ZigZag process to gently perform target guiding without ruining the structure information on the selected pivot. Concretely, our ZigZag process performs one-step denoising and inversion alternately by  $K$  times, where each denoising step provides gradients from the target direction while each inversion step gives a small amount of noise for the next denoising step. Last, a pure editing process is conducted to ensure equal-step inversion and sampling.

Our ZZEdit can be applied painlessly to the existing inversion-based editing methods to boost their performance. As shown in Fig. 1, we compare our ZZEdit with the typical “inversion-then-editing” pipeline using two methods P2P [15] and PnP [43]. Specifically, P2P supports DDIM

inversion and Null-Text inversion (NTI) [26], in which the latter delivers better results by optimizing unconditional textual embeddings. When our ZZEdit are equipped with these editing methods, more elegant editability and fidelity are achieved. To sum up, our main contributions are:

- We provide new empirical insights about locating a structure-preserving while sufficient-for-editing point during the inversion trajectory as the editing pivot.
- We propose a novel zero-shot image editing paradigm named ZZEdit, where a ZigZag process is designed to mildly enhance the target guidance at a suitable pivot.
- Extensive qualitative and quantitative experiments demonstrate that our ZZEdit is versatile across different editing methods, including P2P [15] and PnP [43], which achieves state-of-the-art editing performance.

## 2. Related Works

**Text-driven Image Generation.** Recent years, diffusion models [17, 40] has shown its capacity in text-to-image (T2I) generation. DALLE-2 [33] proposes a two-stage model: a prior generating a CLIP [32] image embedding given a text caption, and a decoder producing an image conditioned on the image embedding. Building on the strength of diffusion models in high-fidelity image generation, Imagen [38] discovers that large frozen language models trained only on text data are effective text encoders for text-to-image generation. Further, to enable diffusion models training on limited computational resources while retaining quality, Stable Diffusion [35] trains models in the latent space of powerful pretrained autoencoders.

**Text-driven Image Editing.** Different from the general text-driven image generation, a group of methods turn the model for single-image editing. SDEdit [24] first adds noise to the input (e.g., stroke painting), then subsequently denoises through the prior from stochastic differential equation (SDE). DiffusionCLIP [21] proposes a text-guided image manipulation method using the pretrained diffusion models and CLIP loss. To further improve the editing fidelity, some approaches require a mask region [1, 2, 27], where the background out of the mask can remain the same while it can be time-consuming for users to provide a mask. Then, for text-only intuitive image editing, DiffEdit [7] and MasaCtrl [6] automatically infer a mask according to the target prompt. P2P [15] and PnP [43] demonstrate that fine-grained control can be achieved by cross-attention layers and manipulating spatial features and their self-attention inside the model respectively. Besides, Imagic [20] and UniTune [44] conduct fine-tuning on Imagen [38] to capture the image-specific appearance, which also does not need edit masks either. Further, Instruct-Pix2Pix [5] and MagicBrush [49] perform editing following human instructions by constructing paired data. Pix2Pix-Zero [29] can perform image-to-image translation with-

out manual prompting. Moreover, another line of techniques proposes to insert new concepts into a pretrained T2I model (e.g., a specified person, bag, cup) for personalize usage [10, 12, 22, 37, 39, 41].

**Inversion in Editing Models.** The commonly-used DDIM inversion scheme [8, 40] conducts DDIM sampling in the reverse direction, which is effective for unconditional generation. When the classifier-free guidance [16] is applied for editing purposes, the accumulated error of DDIM inversion would magnify and lead to a poor reconstruction, thus bringing unsatisfied editing results. To address this, several methods [9, 26] propose to perform optimization on inverted latents, where Null-text inversion (NTI) [26] optimizes the unconditional textual embedding while Prompt-Tuning inversion (PTI) [9] optimizes the conditional embedding. There are also some techniques [13, 19, 45] improve DDIM inversion without fine-tuning.

Different from the above methods, we take a close look at the latent trajectory of the existing “inversion-then-editing” pipeline, which usually takes an approximate-Gaussian latent as the editing pivot. However, we argue that it is usually a suboptimal solution. Without additional training, we propose a new editing paradigm ZZEdit, which enhances editing mildly at a structure-preserving while sufficient-for-editing point, which considers structure and editability in the latent trajectory all at once.

### 3. Preliminary

**Stable Diffusion (SD).** SD [35] trains diffusion models for text-to-image generation in the latent space of an autoencoder  $\mathcal{D}(\mathcal{E}(x))$ . The encoder evaluates the latent feature  $z = \mathcal{E}(x)$  for an input image while the decoder  $\mathcal{D}$  maps the latent representation to the RGB space. In the forward process, the latent input  $z_0$  is perturbed by Gaussian noise gradually, leading to  $z_t$ . To sequentially denoising, a U-Net [36]  $\epsilon_\theta$  containing a series of residual, self-attention, and cross-attention blocks is trained to predict the noise by a L2 loss. Once trained, deterministic DDIM sampling [40] can be applied to accurately reconstruct a given real image:

$$z_{t-1} = \sqrt{\frac{\alpha_{t-1}}{\alpha_t}} z_t + \left( \sqrt{\frac{1}{\alpha_{t-1}} - 1} - \sqrt{\frac{1}{\alpha_t} - 1} \right) \epsilon_\theta(z_t, t, \mathcal{C}), \quad (1)$$

where  $\mathcal{C}$  denotes the text embeddings.

**DDIM Inversion.** DDIM inversion [40] projects an image into a known latent space before reconstruction or editing, which performs DDIM sampling process in a reverse way:

$$z_{t+1} = \sqrt{\frac{\alpha_{t+1}}{\alpha_t}} z_t + \left( \sqrt{\frac{1}{\alpha_{t+1}} - 1} - \sqrt{\frac{1}{\alpha_t} - 1} \right) \epsilon_\theta(z_t, t, \mathcal{C}). \quad (2)$$

The technique is based on the assumption that the ODE process can be reversed in the limit of small steps.

**Classifier-free Guidance (CFG).** To enhance the guidance of the text guidance in text-guided generation, classifier-free guidance [16] is proposed, where both conditioned prediction and unconditioned prediction are performed at each step. The calculation is defined as:

$$\bar{\epsilon}_\theta(z_t, t, \mathcal{C}, \emptyset) = \omega \cdot \epsilon_\theta(z_t, t, \mathcal{C}) + (1 - \omega) \cdot \epsilon_\theta(z_t, t, \emptyset), \quad (3)$$

where  $\emptyset$  is the embeddings of a null text, and  $\omega$  is the guidance scale parameter. Note that DDIM inversion can nearly reconstruct the original image [26], where a slight error is introduced in each step. However, a large guidance scale  $\omega > 1$  is necessary for the editing task, which would magnify such accumulated error [9, 26].

## 4. Methods

Given a source image  $I$  and a target prompt  $\mathcal{P}_{tgt}$ , text-driven image editing tries to achieve two needs: *editability* and *fidelity*. The former aims to change visual content to be consistent with the textual description of  $\mathcal{P}_{tgt}$ , while the latter requires the rest to remain unchanged. In this section, we first analyze the existing “inversion-then-editing” pipeline in Sec. 4.1. Then, the overview of the proposed ZZEdit is given in Sec. 4.2, which first locates a sufficient-for-editing while structure-preserving point as the editing pivot and then performs a mild target guiding process still holding structure information based on this pivot. We elaborate on these two parts in Sec. 4.3 and Sec. 4.4. Our ZZEdit can be applied painlessly in those methods which obey “inversion-then-editing” and improve their performance.

### 4.1. Pilot Analysis

Recent text-only image editing pipeline always directly invert the source image  $I$  for  $T$  steps to obtain an approximately standard Gaussian noise  $z_T$ , from which an edited image is sampled under the guidance of target prompt  $\mathcal{P}_{tgt}$  using CFG. However, *we argue that it is not a good choice to directly invert the input image to a near-Gaussian noise*. Next, we use commonly used DDIM inversion to verify this from the perspective of both *editability* and *fidelity*.

**Editability.** In Fig.2, we divide the T-step process into five parts evenly. At the reconstruction stage of DDIM denoising, the source image  $z_0$  is nearly reconstructed, where the reconstructed latent  $\hat{z}_t$  is approximately equal to the inverted latent  $z_t$  (i.e.,  $z_t \approx \hat{z}_t$ ). Then, we attempt to quantitatively measure the target guidance degree for the different inverted latent  $z_t$ , where  $t \in [\frac{1}{5}T, \frac{2}{5}T, \frac{3}{5}T, \frac{4}{5}T, T]$ .

We use CFG scale  $\omega = 7.5$  for target editing, where  $\frac{1}{5}T$ -step sampling is conducted on  $z_t$ , yielding  $\tilde{z}_{t-\frac{1}{5}T}$  as  $\tilde{z}_0, \tilde{z}_{\frac{1}{5}T}, \tilde{z}_{\frac{2}{5}T}, \tilde{z}_{\frac{3}{5}T}$ , and  $\tilde{z}_{\frac{4}{5}T}$ , respectively. Here, since  $z_t \approx \hat{z}_t$ , we can distinguish editing trajectories of different  $z_t$  with  $\hat{z}_t$ : ①  $\hat{z}_{\frac{1}{5}T} \rightarrow \tilde{z}_0^1$ , ②  $\hat{z}_{\frac{2}{5}T} \rightarrow \tilde{z}_{\frac{1}{5}T}^2 \rightarrow \tilde{z}_0^2$ , ③  $\hat{z}_{\frac{3}{5}T} \rightarrow \tilde{z}_{\frac{2}{5}T}^3 \rightarrow \tilde{z}_{\frac{1}{5}T}^3 \rightarrow \tilde{z}_0^3$ , ④  $\hat{z}_{\frac{4}{5}T} \rightarrow \tilde{z}_{\frac{3}{5}T}^4 \rightarrow \tilde{z}_{\frac{2}{5}T}^4 \rightarrow \tilde{z}_{\frac{1}{5}T}^4 \rightarrow \tilde{z}_0^4$ .



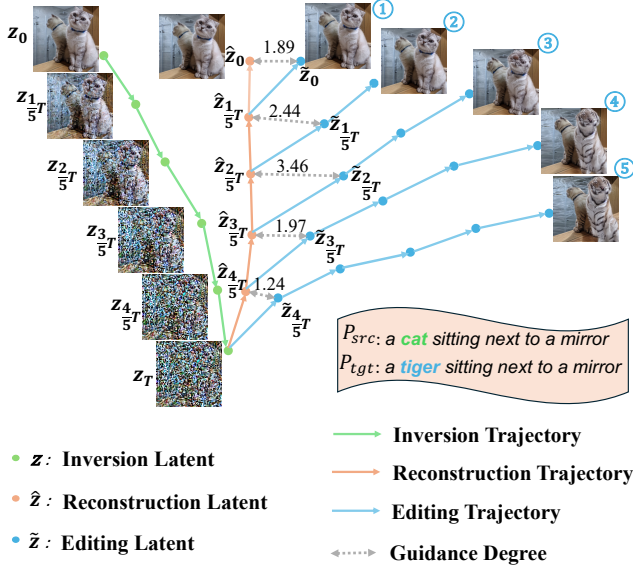


Figure 2. Pilot analysis on the “inversion-then-editing” pipeline, which takes source prompt  $\mathcal{P}_{src}$ , target prompt  $\mathcal{P}_{tgt}$ , and a clean latent  $z_0$  as input. In the DDIM inversion trajectory,  $z_0$  is inverted into a near-Gaussian latent  $z_T$  using source prompt  $\mathcal{P}_{src}$  and UNet  $\epsilon_\theta$ . At the reconstruction stage of DDIM denoising,  $\hat{z}_t \approx z_t$ . At the editing stage of the DDIM denoising, we use  $\|\hat{z}_t - z_t\|$  to approximately measure the guidance degree of  $\mathcal{P}_{tgt}$  for different reconstructed  $\hat{z}_t$ , which shows the intermediate-inverted  $z_t$  has considerable (or greater) editability as the fully-inverted  $z_T$ .

and  $\textcircled{5} z_T \rightarrow \tilde{z}_{\frac{4}{5}T}^5 \rightarrow \tilde{z}_{\frac{3}{5}T}^5 \rightarrow \tilde{z}_{\frac{2}{5}T}^5 \rightarrow \tilde{z}_{\frac{1}{5}T}^5 \rightarrow \tilde{z}_0^5$ . We omit these superscripts in Fig.2 for simplicity. Next, we can measure the deviation of the reconstructed  $\hat{z}_{t-\frac{1}{5}T}$  and target-guided  $\tilde{z}_{t-\frac{1}{5}T}$  by calculating the norm of difference between them (i.e.,  $\|\tilde{z}_{t-\frac{1}{5}T} - \hat{z}_{t-\frac{1}{5}T}\|$ ). Such a measurement can be regarded as a statistical average result using  $\frac{1}{5}T$  steps, which shows the guiding degree of the target prompt  $\mathcal{P}_{tgt}$  to different  $z_t$ , where  $t \in [\frac{1}{5}T, \frac{2}{5}T, \frac{3}{5}T, \frac{4}{5}T, T]$ .

It turns out the largest guidance degree occurs in the editing trajectory of  $\textcircled{3}$  in our pilot analysis. In this way, a general discovery can be obtained: intermediate-inverted  $z_t$  is capable of providing considerable (or greater) response level to the target prompt  $\mathcal{P}_{tgt}$  as the fully-inverted  $z_T$ , proving the editability of intermediate-inverted  $z_t$ .

**Fidelity.** DDIM inversion introduces a slight error at each step, and such accumulated errors would be magnified under a large CFG scale  $\omega$  [26]. Thus, using  $z_T$  for subsequent denoising would inevitably bring more reconstruction errors than intermediate-inverted ones, hindering the fidelity and leading to a significantly different image.

Summing up, intermediate-inverted latents can provide a better trade-off between editability and fidelity than fully-inverted  $z_T$  since the latter barely lost all structure fidelity for subsequent reconstruction and editing.

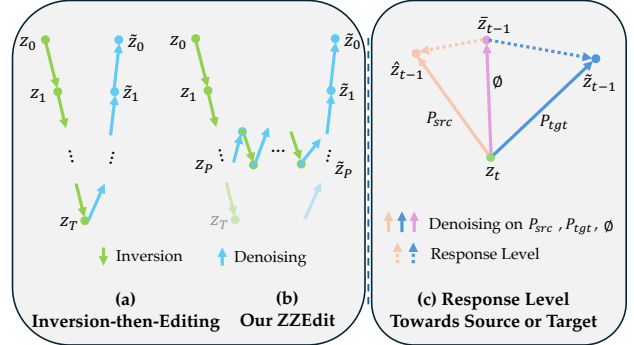


Figure 3. Left: (a) The trajectory of the “inversion-then-editing” pipeline, which inverts  $z_0$  to  $z_T$  using  $\mathcal{P}_{src}$ , and then performs denoising under  $\mathcal{P}_{tgt}$ . (b) The trajectory of our ZZEdit, where we first locate a sufficient-for-editing while structure-preserving point (marked as  $P$ ) on the inversion trajectory as the editing pivot, and then use a ZigZag process to mildly guide the latent towards the target. Afterwards, a pure denoising process is leveraged for the equal step of inversion and denoising. Right: (c) Illustration of the response of the inverted latent  $z_t$  towards  $\mathcal{P}_{src}$ , null text  $\emptyset$ , and  $\mathcal{P}_{tgt}$ , which are represented with dotted lines. The more the denoised latent deviates from that of  $\emptyset$ , the greater the response.

## 4.2. Overview of The Proposed ZZEdit

Considering the potential good property of intermediate-inverted latents, this paper attempts to *mildly strengthens the target guidance on a sufficient-for-editing while structure-preserving latent*. Specifically, as seen in the left part of Fig. 3, we propose a new editing paradigm ZZEdit, which consists of three steps:

- (i) We attempt to locate an optimal point in inversion trajectory as the editing pivot, which is detailed in Sec. 4.3.
- (ii) A mild guiding process, named ZigZag process is proposed to enhance target guidance at the pivot. Specifically, it consists of alternately performing one-step denoising and one-step inversion, which is elaborated in Sec. 4.4.
- (iii) The remaining comprises a diffusion process guided by the target prompt to achieve equal-step inversion and sampling. Note that when equipping the existing editing method with our ZZEdit, the denoising process needs to retain the characteristics of the method, such as P2P [15] injecting cross-attention maps and PnP [43] injecting self-attention maps. We summarize applying our ZZEdit to the existing text-driven image editing methods in Alg. 1.

## 4.3. Towards An Optimal Pivot During Inversion

We argue that a qualified intermediate-inverted latent for the editing pivot should consider both editability and fidelity. We ensure the former by seeking a sufficient-for-editing point which has a larger response towards the target prompt  $\mathcal{P}_{tgt}$  than source prompt  $\mathcal{P}_{src}$ . The latter is naturally guaranteed by fewer adding-noise steps. As seen in the right part of Fig. 3, given an intermediate-inverted  $z_t$ , we



---

**Algorithm 1:** ZZEdit for Zero-shot Image Editing

---

**Input:** The inverted latents  $\{z_0, z_1, \dots, z_T\}$ , source prompt  $\mathcal{P}_{src}$ , and target prompt  $\mathcal{P}_{tgt}$

**Output:** An edited image or latent embedding  $\tilde{z}_0$

---

```
1 Part I: Locating A Structure-preserving While
  Sufficient-for-editing Step  $P$  as The Editing Pivot
2 for  $t = 0 \rightarrow T$  do
  // Using Eqn. 1 for Single-step
  Denoising With  $\mathcal{P}_{src}$ ,  $\mathcal{P}_{tgt}$ , and  $\emptyset$ 
3    $\hat{z}_{t-1} \leftarrow \epsilon_\theta(z_t, t, \mathcal{C}_{src});$ 
    $\tilde{z}_{t-1} \leftarrow \epsilon_\theta(z_t, t, \mathcal{C}_{tgt});$ 
    $\bar{z}_{t-1} \leftarrow \epsilon_\theta(z_t, t, \emptyset);$ 
4   if  $\|\tilde{z}_{t-1} - \bar{z}_{t-1}\| > \|\hat{z}_{t-1} - \bar{z}_{t-1}\|$  then
5     break
6   end
7 end
8 Return  $t$ 
9 Part II: ZigZag Process
10 for  $t = P$  do
11   ZigZag Process alternately executes one-step
   denoising (Eqn. 6) and inversion (Eqn. 5);
12 end
13 Part III: Continuous Denoising Process
14 for  $t = P \rightarrow 0$  do
15   Denoising step equipped with existing image
   editing techniques such as P2P and PnP;
16 end
```

---

can use Eqn. 1 for DDIM sampling to obtain the denoised latent  $\hat{z}_{t-1}$ ,  $\bar{z}_{t-1}$ , and  $\tilde{z}_{t-1}$  under the source prompt  $\mathcal{P}_{src}$ , null text  $\emptyset$ , and target prompt  $\mathcal{P}_{tgt}$  separately:

$$\hat{z}_{t-1} \leftarrow \epsilon_\theta(z_t, t, \mathcal{C}_{src}), \tilde{z}_{t-1} \leftarrow \epsilon_\theta(z_t, t, \mathcal{C}_{tgt}), \bar{z}_{t-1} \leftarrow \epsilon_\theta(z_t, t, \emptyset).$$

Then, we measure the response level towards the target prompt  $\mathcal{P}_{tgt}$  as  $\|\tilde{z}_{t-1} - \bar{z}_{t-1}\|$  and that towards the source prompt  $\mathcal{P}_{src}$  as  $\|\hat{z}_{t-1} - \bar{z}_{t-1}\|$ . Here, the denoised latent  $\bar{z}_{t-1}$  using  $\emptyset$  is used as an anchor. The more the denoised latent deviates from that of  $\emptyset$ , the greater the response.

Generally speaking, the latent  $z_t$  with low-degree inversion would be more responsive to source prompt  $\mathcal{P}_{src}$  due to limited corruption. As the inversion deepens, we can easily find those points whose response to target prompt  $\mathcal{P}_{tgt}$  is greater than that to source prompt, which is described as:

$$\|\tilde{z}_{t-1} - \bar{z}_{t-1}\| > \|\hat{z}_{t-1} - \bar{z}_{t-1}\|. \quad (4)$$

For simplicity, we only locate the *first* point during inversion which has a larger target response as our editing pivot. We mark the satisfied step  $t$  as  $P \in [0, 1, \dots, T]$ . We show the pseudo algorithm in part I of Alg. 1.

Note that the response calculation here is similar to that in the pilot experiment ( $\|\tilde{z}_{t-\frac{1}{5}T} - \hat{z}_{t-\frac{1}{5}T}\|$ ). The differences are: (i) single-step denoising rather than  $\frac{1}{5}T$ -step one here for fast locating the editing pivot; (ii) the reconstructed latent  $\bar{z}_{t-1}$  is used as an anchor to evaluate the response level towards  $\mathcal{P}_{tgt}$  and  $\mathcal{P}_{src}$  separately, while  $\|\tilde{z}_{t-1} - \hat{z}_{t-1}\|$  merely reflects the guidance degree of  $\mathcal{P}_{tgt}$  for  $z_t$ .

#### 4.4. Mild Guiding: ZigZag Process

To mildly deepen editing without ruining the fidelity of previously located pivot, we propose a ZigZag process, which alternately executes one-step sampling and inversion.

**Mild Guiding.** As illustrated in Fig. 3, our ZigZag process is started after a  $P$ -step inversion. Formally, a full ZigZag process includes  $K$  denoising steps and  $K$  inversion steps, which are conducted alternately. We treat a denoising step and inversion step as a union, making ZigZag process consist of  $K$  unions. The inversion step of  $k$ -th union is:

$$z_t^k = \sqrt{\frac{\alpha_t}{\alpha_{t-1}}} z_{t-1}^k + \left( \sqrt{\frac{1}{\alpha_t} - 1} - \sqrt{\frac{1}{\alpha_{t-1}} - 1} \right) \epsilon_\theta(z_{t-1}^k, t, \mathcal{C}_{src}), \quad (5)$$

where  $k \in \{1, 2, \dots, K\}$ . Then, the denoising step of  $(k+1)$ -th union in ZigZag process is:

$$z_{t-1}^{k+1} = \sqrt{\frac{\alpha_{t-1}}{\alpha_t}} z_t^k + \left( \sqrt{\frac{1}{\alpha_{t-1}} - 1} - \sqrt{\frac{1}{\alpha_t} - 1} \right) \epsilon_\theta(z_t^k, t, \mathcal{C}_{tgt}), \quad (6)$$

Substituting Eqn. 5 into Eqn. 6, we can obtain:

$$z_{t-1}^{k+1} = z_{t-1}^k + \left( \sqrt{\frac{1}{\alpha_{t-1}} - 1} - \sqrt{\frac{1}{\alpha_t} - 1} \right) \cdot \eta, \quad (7)$$

$$\eta = \epsilon_\theta(z_t^k, t, \mathcal{C}_{tgt}) - \epsilon_\theta(z_{t-1}^k, t-1, \mathcal{C}_{src}), \quad (8)$$

where  $\left( \sqrt{\frac{1}{\alpha_{t-1}} - 1} - \sqrt{\frac{1}{\alpha_t} - 1} \right) > 0$  according to noise schedule of diffusion models [40]. Thus, compared with the inverted latent in  $k$ -th union (i.e.,  $z_{t-1}^k$ ), the denoising latent in  $(k+1)$ -th union (i.e.,  $z_{t-1}^{k+1}$ ) would move towards target. Overall, each denoising step in ZigZag process provides gradients from  $\mathcal{P}_{tgt}$  while each inversion step gives a small amount of noise for the next denoising step.

**ZigZag Steps.** For a fair comparison, we use the same steps of inversion and sampling with the typical “inversion-then-editing” pipeline to determine the number of ZigZag steps. That is,  $P + K = T$ . Then, when the located editing pivot reaches  $T$  steps (i.e.,  $P = T$ ), we make ZZEdit degenerate to the typical “inversion-then-editing” pipeline. Besides, to flexibly control the number of ZigZag steps, we additionally introduce a hyper-parameter  $a$  as:

$$K = a \cdot (T - P), \quad (9)$$

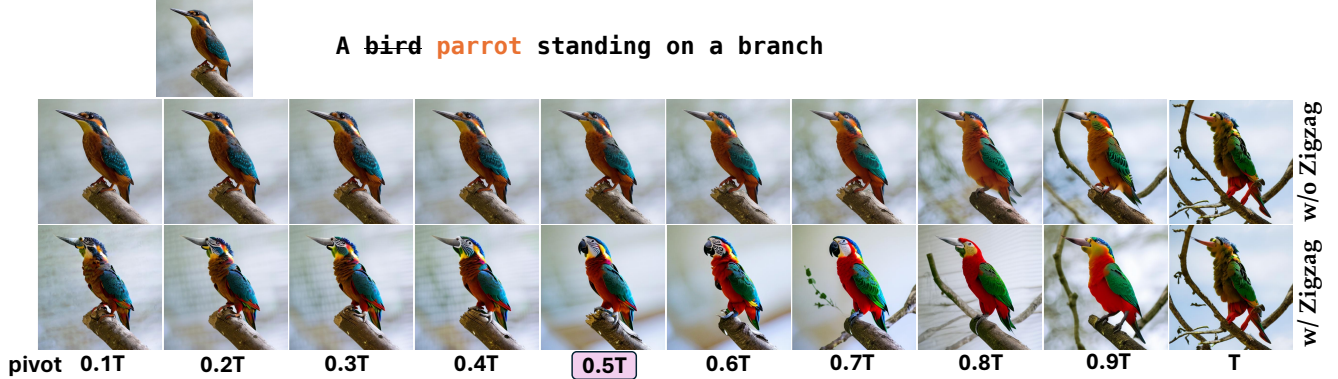


Figure 4. Ablation study of ZZEdit on P2P [15] w/ DDIM inversion. The first row displays the editing results when different points on the inversion trajectory are leveraged as the editing pivot, where no ZigZag process is equipped. Then, the second row shows the performance of using the ZigZag process additionally. Our method first locates a suitable pivot (marked with purple) and then mildly performs target guiding, which yields the most elegant editing results.

Method		Structure	Background Preservation			CLIP Similarity		
		L2 ↓	PSNR ↑	LPIPS ↓	MSE ↓	SSIM ↑	Whole ↑	Edited ↑
<b>P2P+DDIM Baseline</b>		69.41	17.88	208.37	219.11	71.30	25.01	22.44
<i>w/ Pivot</i>	<i>w/o ZigZag (a = 0)</i>	<b>22.60</b>	<b>23.71</b>	<b>107.01</b>	<b>68.27</b>	<b>79.60</b>	24.43	21.52
	<i>w/ ZigZag (a = 0.2)</i>	27.50	22.97	116.02	82.79	78.71	24.70	22.04
	<i>w/ ZigZag (a = 0.6)</i>	28.26	22.48	122.36	87.26	77.94	25.07	22.14
	<i>w/ ZigZag (a = 1)</i>	31.99	21.92	131.57	96.95	76.98	<b>25.29</b>	<b>22.47</b>
<b>Random Pivot w/ ZigZag (a = 1)</b>		25.84	24.07	105.36	81.43	79.56	24.76	21.84

Table 1. Quantitative ablation study on our ZigZag process with P2P [15] w/ DDIM inversion. We mark the best results in the ZigZag process in bold. We also provide the performance of using random editing pivot, where a standard ZigZag process is equipped.

where  $a \in [0, 1]$ . When  $a = 0$ , a continuous  $P$ -step sampling is performed from the located editing pivot without ZigZag process. When  $a = 1$ , our ZZEdit realizes  $T$  inversion and sampling steps separately, consuming the same UNet operations as the “inversion-then-editing” pipeline.

## 5. Experiment

### 5.1. Experimental setup

**Implementation Details.** All experiments is conducted on a single Tesla A100 GPU using PyTorch [30]. Following [43], we use 50 steps as DDIM schedule and the classifier-free guidance of 7.5 for editing. Besides, we use the official code of SD 1.5. For a fair comparison, we adopt the same cross-attention injection parameters and self-attention injection parameters as P2P [15] and PnP [43]. In practice, to save time and computation, when looking for the editing pivot, we only search from  $[0.4T, 0.5T, \dots, T]$ , rather than  $[0, 1, \dots, T]$ . The reasons are: (1) low-degree inversion generally struggles for sufficient editability and (2) there is no need to look up each step.

**Evaluation Metrics.** We use the PIE-Bench dataset [19] to evaluate our method. The editing results are evaluated on three aspects: structure distance [42], background preservation covering PSNR [18], SSIM [46], MSE, and LPIPS [51],

and editing consistency of the whole image and regions in the editing mask, denoted as CLIP similarity [47].

### 5.2. Ablation Studies

We ablate several key designs of our ZZEdit paradigm, which aims to answer the following questions. **Q1:** What is the difference between using different points on the inversion trajectory as the editing pivot? **Q2:** Could our ZZEdit locate a suitable pivot, which maintains both structure and editability? **Q3:** Could the proposed ZigZag process enhance the target guidance at the suitable pivot?

**Different Editing Pivot in ZZEdit.** In Fig. 4, we answer the first question by applying our ZZEdit on P2P [15] w/ DDIM inversion and report the performance of selecting the value of  $P$  from  $[0.1T, 0.2T, \dots, 0.9T, T]$  for different inversion degree. The first row uses  $P$ -step inversion and  $P$ -step sampling without the ZigZag process. The second row displays the results of ZigZag process equipped for different editing pivot (inversion degree), where each result in the second row satisfies  $P + K = T$  to make the UNet operations are same with the “inversion-then-editing” baseline.

From the first row, we can observe that the target prompt has different guiding abilities to different points on the inversion trajectory. For example, when we choose  $[0.1T, 0.2T, 0.3T, 0.4T]$  as the editing pivot, structure fi-



Figure 5. Qualitative ablation on our ZigZag process with P2P [15] and PnP [43], which mildly enhances the guidance at a suitable pivot.

Method		Structure	Background Preservation				CLIP Similarity	
Editing	Inv Setting	L2 ↓	PSNR ↑	LPIPS ↓	MSE ↓	SSIM ↑	Whole ↑	Edited ↑
P2P	DDIM	69.41	17.88	208.37	219.11	71.30	25.01	22.44
	NTI	13.72	27.05	60.74	35.89	84.27	24.75	21.86
	PTI	16.17	26.21	69.01	39.73	83.40	24.61	21.87
	Pnp_inv	11.65	27.22	54.55	32.86	84.76	25.02	22.10
	ZZEdit (w/ DDIM)	31.99	21.92	131.57	96.95	76.98	<b>25.29</b>	<b>22.47</b>
	ZZEdit (w/ NTI)	<b>11.47</b>	<b>27.42</b>	<b>53.92</b>	<b>31.23</b>	<b>84.98</b>	24.95	22.01
PnP	DDIM	28.22	22.28	113.46	83.64	79.05	25.41	22.55
	Pnp_inv	24.29	22.46	106.06	80.45	79.68	25.41	22.62
	ZZEdit (w/ DDIM)	<b>23.49</b>	<b>24.55</b>	<b>86.61</b>	<b>55.04</b>	<b>82.18</b>	<b>25.43</b>	<b>22.91</b>

Table 2. Comparison between ZZEdit and “inversion-then-editing” pipeline on P2P [15] and PnP [43] under different inversion settings: DDIM [40], NTI [26], PTI [9], and Pnp inversion [19].

delity is maintained well, but editability is poor. It demonstrates that a low-degree inversion struggles to bring sufficient editability. Besides, we notice that when using high-degree inversion (e.g.,  $[0.8T, 0.9T, T]$ ), the results deliver satisfactory editability but an unpleasing background fidelity since accumulated reconstruction errors. As for the second row, we equip ZigZag process at different editing pivots. Note that for those low-degree inversion latents, using the ZigZag process also shows limited editability. Fortunately, our method first finds a structure-preserving while sufficient-for-editing point (marked in purple), and then performs mild guiding with the ZigZag process, which yields the best editing performance. We also use GPT-4V (ision) system [28] to evaluate Fig. 4 in our supplement.

**The Effectiveness of Our Located Pivot.** We answer the second question by comparing with the results of selecting an editing pivot randomly from  $[0.1T, 0.2T, \dots, 0.9T, T]$ , where the standard ZigZag process ( $a = 1$ ) is equipped.

As shown in Tab. 1, compared with the P2P baseline, although “random pivot w/ ZigZag” can achieve excellent background and structure preservation, but its editing consistency is poor. In contrast, our located pivot with the standard ZigZag process ( $a = 1$ ) achieves much higher CLIP scores, which proves the effectiveness of the editing pivot located in our ZZEdit. Besides, we also give the distribution of the editing pivot in our ZZEdit on the PIE-Bench dataset [19] in our supplement.

**The Effectiveness of The ZigZag Process.** We answer the third question by using different ZigZag steps on a suitable editing pivot, which makes  $a$  in Eq. 9 take the value from  $\{0, 0.2, 0.6, 1\}$ . Fig. 5 shows a qualitative comparison on different baselines. Our ZZEdit can mildly approach the editing purpose through the increasing number of ZigZag steps while still holding a satisfying background. We also provide a quantitative experiment in Tab. 1. When no ZigZag steps are employed ( $a = 0$ ), the best back-





Figure 6. Visualization results of different editing techniques. From left to right: source image, P2P [15] w/ DDIM inversion, our ZZEdit applied on P2P w/ DDIM inversion, P2P w/ Null-text inversion, our ZZEdit applied on P2P w/ Null-text inversion, PnP [43] w/ DDIM inversion, our ZZEdit applied on PnP w/ DDIM inversion, Pix2Pix-Zero [29], Masactrl [6], MagicBrush [49].

ground and structure can be obtained. However, it cannot achieve pleasing editing consistency. Besides, when we equip the ZigZag process, the gradual increase of ZigZag steps ( $a = 0.2, 0.6, \text{ and } 1$ ) can improve editing consistency. The quantitative ablations on the ZigZag process with P2P w/ NTI and PnP w/ DDIM inversion are in our supplement.

### 5.3. Quantitative Results

To prove the superiority of our ZZEdit, we compare it with P2P [15] and PnP [43] under different inversion settings. As seen in Tab. 2, when applying ZZEdit to P2P or PnP, all results of background, structure, and editing consistency are boosted steadily. Besides, PnP w/ ZZEdit outperforms the PnP w/ Pnp inversion clearly. Further, P2P + NTI w/ ZZEdit yields a comparable performance with PnP w/ Pnp inversion. It also shows the superiority of our method.

### 5.4. Qualitative Results

In Fig. 6, we show a qualitative comparison with the current editing methods, including P2P [15] w/ DDIM inversion or NTI, PnP [43] w/ DDIM inversion, Pix2Pix-Zero [29], MagicBrush [49], and Masactrl [6]. The editing scenario

here includes attribute editing, object replacement, style transfer and background editing. Our ZZEdit paradigm can consistently improve the performance of P2P and PnP. Compared with other state-of-the-art methods, our ZZEdit shows its superiority through better background fidelity and editing consistency. More comparisons of editing results can be found in the supplement.

## 6. Conclusion

We presented a novel zero-shot image editing paradigm, dubbed ZZEdit. Based on the observation that intermediate-inverted latents can deliver a better trade-off between editability and fidelity, we proposed to use a sufficient-for-editing while structure-preserving point rather than  $z_T$  as the editing pivot. Then, a ZigZag process was designed to execute sampling and inversion alternately, which mildly approaches the target based on this pivot. Finally, we conducted a sampling process solely to keep the same-step inversion and sampling. Comprehensive experiments have shown that we achieve outstanding outcomes across a broad spectrum of text-driven image editing methods.

## References

- [1] Omri Avrahami, Dani Lischinski, and Ohad Fried. Blended diffusion for text-driven editing of natural images. In *CVPR*, pages 18208–18218, 2022. 2
- [2] Omri Avrahami, Ohad Fried, and Dani Lischinski. Blended latent diffusion. *ACM Transactions on Graphics (TOG)*, 42(4):1–11, 2023. 2
- [3] Omri Avrahami, Thomas Hayes, Oran Gafni, Sonal Gupta, Yaniv Taigman, Devi Parikh, Dani Lischinski, Ohad Fried, and Xi Yin. Spatext: Spatio-textual representation for controllable image generation. In *CVPR*, pages 18370–18380, 2023. 2
- [4] Omer Bar-Tal, Dolev Ofri-Amar, Rafail Fridman, Yoni Kasten, and Tali Dekel. Text2live: Text-driven layered image and video editing. In *ECCV*, pages 707–723. Springer, 2022. 2
- [5] Tim Brooks, Aleksander Holynski, and Alexei A Efros. Instructpix2pix: Learning to follow image editing instructions. In *CVPR*, pages 18392–18402, 2023. 2
- [6] Mingdeng Cao, Xintao Wang, Zhongang Qi, Ying Shan, Xiaoohu Qie, and Yinqiang Zheng. Masactrl: Tuning-free mutual self-attention control for consistent image synthesis and editing. In *ICCV*, pages 22560–22570, 2023. 2, 8
- [7] Guillaume Couairon, Jakob Verbeek, Holger Schwenk, and Matthieu Cord. Diffedit: Diffusion-based semantic image editing with mask guidance. *arXiv preprint arXiv:2210.11427*, 2022. 2
- [8] Prafulla Dhariwal and Alexander Nichol. Diffusion models beat gans on image synthesis. *NeurIPS*, 34:8780–8794, 2021. 3
- [9] Wenkai Dong, Song Xue, Xiaoyue Duan, and Shumin Han. Prompt tuning inversion for text-driven image editing using diffusion models. In *ICCV*, pages 7430–7440, 2023. 2, 3, 7
- [10] Ziyi Dong, Pengxu Wei, and Liang Lin. Dreamartist: Towards controllable one-shot text-to-image generation via contrastive prompt-tuning. *arXiv preprint arXiv:2211.11337*, 2022. 3
- [11] Oran Gafni, Adam Polyak, Oron Ashual, Shelly Sheynin, Devi Parikh, and Yaniv Taigman. Make-a-scene: Scene-based text-to-image generation with human priors. In *ECCV*, pages 89–106. Springer, 2022. 2
- [12] Rinon Gal, Yuval Alaluf, Yuval Atzmon, Or Patashnik, Amit H Bermano, Gal Chechik, and Daniel Cohen-Or. An image is worth one word: Personalizing text-to-image generation using textual inversion. *arXiv preprint arXiv:2208.01618*, 2022. 3
- [13] Daniel Garibi, Or Patashnik, Andrey Voynov, Hadar Averbuch-Elor, and Daniel Cohen-Or. Renoise: Real image inversion through iterative noising. *arXiv preprint arXiv:2403.14602*, 2024. 3
- [14] Shuyang Gu, Dong Chen, Jianmin Bao, Fang Wen, Bo Zhang, Dongdong Chen, Lu Yuan, and Baining Guo. Vector quantized diffusion model for text-to-image synthesis. In *CVPR*, pages 10696–10706, 2022. 1
- [15] Amir Hertz, Ron Mokady, Jay Tenenbaum, Kfir Aberman, Yael Pritch, and Daniel Cohen-Or. Prompt-to-prompt image editing with cross attention control. *arXiv preprint arXiv:2208.01626*, 2022. 1, 2, 4, 6, 7, 8
- [16] Jonathan Ho and Tim Salimans. Classifier-free diffusion guidance. *arXiv preprint arXiv:2207.12598*, 2022. 3
- [17] Jonathan Ho, Ajay Jain, and Pieter Abbeel. Denoising Diffusion Probabilistic Models. *NeurIPS*, 33:6840–6851, 2020. 2
- [18] Quan Huynh-Thu and Mohammed Ghanbari. The accuracy of psnr in predicting video quality for different video scenes and frame rates. *Telecommunication Systems*, 49:35–48, 2012. 6
- [19] Xuan Ju, Ailing Zeng, Yuxuan Bian, Shaoteng Liu, and Qiang Xu. Pnp inversion: Boosting diffusion-based editing with 3 lines of code. *ICLR*, 2024. 2, 3, 6, 7, 1
- [20] Bahjat Kawar, Shiran Zada, Oran Lang, Omer Tov, Huiwen Chang, Tali Dekel, Inbar Mosseri, and Michal Irani. Imagic: Text-based real image editing with diffusion models. In *CVPR*, pages 6007–6017, 2023. 2
- [21] Gwanghyun Kim, Taesung Kwon, and Jong Chul Ye. Diffusionclip: Text-guided diffusion models for robust image manipulation. In *CVPR*, pages 2426–2435, 2022. 2
- [22] Nupur Kumari, Bingliang Zhang, Richard Zhang, Eli Shechtman, and Jun-Yan Zhu. Multi-concept customization of text-to-image diffusion. In *CVPR*, pages 1931–1941, 2023. 3
- [23] Yuheng Li, Haotian Liu, Qingyang Wu, Fangzhou Mu, Jianwei Yang, Jianfeng Gao, Chunyuan Li, and Yong Jae Lee. Gligen: Open-set grounded text-to-image generation. In *CVPR*, pages 22511–22521, 2023. 2
- [24] Chenlin Meng, Yutong He, Yang Song, Jiaming Song, Jiajun Wu, Jun-Yan Zhu, and Stefano Ermon. Sedit: Guided image synthesis and editing with stochastic differential equations. *ICLR*, 2022. 2
- [25] Ron Mokady, Omer Tov, Michal Yarom, Oran Lang, Inbar Mosseri, Tali Dekel, Daniel Cohen-Or, and Michal Irani. Self-distilled stylegan: Towards generation from internet photos. In *ACM SIGGRAPH 2022 Conference Proceedings*, pages 1–9, 2022. 2
- [26] Ron Mokady, Amir Hertz, Kfir Aberman, Yael Pritch, and Daniel Cohen-Or. Null-text inversion for editing real images using guided diffusion models. In *CVPR*, pages 6038–6047, 2023. 1, 2, 3, 4, 7
- [27] Alex Nichol, Prafulla Dhariwal, Aditya Ramesh, Pranav Shyam, Pamela Mishkin, Bob McGrew, Ilya Sutskever, and Mark Chen. Glide: Towards photorealistic image generation and editing with text-guided diffusion models. *arXiv preprint arXiv:2112.10741*, 2021. 2
- [28] OpenAI. *GPT-4V(ision) system card*. URL <https://openai.com/research/gpt-4v-system-card>, 2023. 7, 1, 2, 5, 6
- [29] Gaurav Parmar, Krishna Kumar Singh, Richard Zhang, Yijun Li, Jingwan Lu, and Jun-Yan Zhu. Zero-shot image-to-image translation. In *ACM SIGGRAPH 2023 Conference Proceedings*, pages 1–11, 2023. 2, 8
- [30] Adam Paszke, Sam Gross, Francisco Massa, Adam Lerer, James Bradbury, Gregory Chanan, Trevor Killeen, Zeming Lin, Natalia Gimelshein, Luca Antiga, et al. Pytorch:

- An imperative style, high-performance deep learning library. *NeurIPS*, 32, 2019. 6
- [31] Can Qin, Shu Zhang, Ning Yu, Yihao Feng, Xinyi Yang, Yingbo Zhou, Huan Wang, Juan Carlos Niebles, Caiming Xiong, Silvio Savarese, et al. Unicontrol: A unified diffusion model for controllable visual generation in the wild. *NeurIPS*, 2023. 2
- [32] Alec Radford, Jong Wook Kim, Chris Hallacy, Aditya Ramesh, Gabriel Goh, Sandhini Agarwal, Girish Sastry, Amanda Askell, Pamela Mishkin, Jack Clark, et al. Learning transferable visual models from natural language supervision. In *ICML*, pages 8748–8763. PMLR, 2021. 2
- [33] Aditya Ramesh, Prafulla Dhariwal, Alex Nichol, Casey Chu, and Mark Chen. Hierarchical text-conditional image generation with clip latents. *arXiv preprint arXiv:2204.06125*, 1(2):3, 2022. 1, 2
- [34] Aditya Ramesh, Prafulla Dhariwal, Alex Nichol, Casey Chu, and Mark Chen. Hierarchical text-conditional image generation with clip latents. *arXiv preprint arXiv:2204.06125*, 2022. 2
- [35] Robin Rombach, Andreas Blattmann, Dominik Lorenz, Patrick Esser, and Björn Ommer. High-resolution image synthesis with latent diffusion models. In *CVPR*, pages 10684–10695, 2022. 1, 2, 3
- [36] Olaf Ronneberger, Philipp Fischer, and Thomas Brox. U-net: Convolutional networks for biomedical image segmentation. In *Medical Image Computing and Computer-Assisted Intervention—MICCAI 2015: 18th International Conference, Munich, Germany, October 5-9, 2015, Proceedings, Part III 18*, pages 234–241. Springer, 2015. 3
- [37] Nataniel Ruiz, Yuanzhen Li, Varun Jampani, Yael Pritch, Michael Rubinstein, and Kfir Aberman. Dreambooth: Fine tuning text-to-image diffusion models for subject-driven generation. In *CVPR*, pages 22500–22510, 2023. 3
- [38] Chitwan Saharia, William Chan, Saurabh Saxena, Lala Li, Jay Whang, Emily L Denton, Kamyar Ghasemipour, Raphael Gontijo Lopes, Burcu Karagol Ayan, Tim Salimans, et al. Photorealistic text-to-image diffusion models with deep language understanding. *NeurIPS*, 35:36479–36494, 2022. 1, 2
- [39] James Seale Smith, Yen-Chang Hsu, Lingyu Zhang, Ting Hua, Zsolt Kira, Yilin Shen, and Hongxia Jin. Continual diffusion: Continual customization of text-to-image diffusion with c-lora. *arXiv preprint arXiv:2304.06027*, 2023. 3
- [40] Jiaming Song, Chenlin Meng, and Stefano Ermon. Denoising diffusion implicit models. *arXiv preprint arXiv:2010.02502*, 2020. 1, 2, 3, 5, 7
- [41] Yoad Tewel, Rinon Gal, Gal Chechik, and Yuval Atzmon. Key-locked rank one editing for text-to-image personalization. In *ACM SIGGRAPH 2023 Conference Proceedings*, pages 1–11, 2023. 3
- [42] Narek Tumanyan, Omer Bar-Tal, Shai Bagon, and Tali Dekel. Splicing vit features for semantic appearance transfer. In *CVPR*, pages 10748–10757, 2022. 6
- [43] Narek Tumanyan, Michal Geyer, Shai Bagon, and Tali Dekel. Plug-and-play diffusion features for text-driven image-to-image translation. In *CVPR*, pages 1921–1930, 2023. 1, 2, 4, 6, 7, 8
- [44] Dani Valevski, Matan Kalman, Yossi Matias, and Yaniv Leviathan. Unitune: Text-driven image editing by fine tuning an image generation model on a single image. *arXiv preprint arXiv:2210.09477*, 2(3):5, 2022. 2
- [45] Bram Wallace, Akash Gokul, and Nikhil Naik. Edict: Exact diffusion inversion via coupled transformations. In *CVPR*, pages 22532–22541, 2023. 3
- [46] Zhou Wang, Alan C Bovik, Hamid R Sheikh, and Eero P Simoncelli. Image quality assessment: from error visibility to structural similarity. *IEEE transactions on image processing*, 13(4):600–612, 2004. 6
- [47] Chenfei Wu, Lun Huang, Qianxi Zhang, Binyang Li, Lei Ji, Fan Yang, Guillermo Sapiro, and Nan Duan. Godiva: Generating open-domain videos from natural descriptions. *arXiv preprint arXiv:2104.14806*, 2021. 6
- [48] Jiahui Yu, Yuanzhong Xu, Jing Yu Koh, Thang Luong, Gungjan Baid, Zirui Wang, Vijay Vasudevan, Alexander Ku, Yinfei Yang, Burcu Karagol Ayan, et al. Scaling autoregressive models for content-rich text-to-image generation. *arXiv preprint arXiv:2206.10789*, 2(3):5, 2022. 1
- [49] Kai Zhang, Lingbo Mo, Wenhui Chen, Huan Sun, and Yu Su. Magicbrush: A manually annotated dataset for instruction-guided image editing. *Advances in Neural Information Processing Systems*, 36, 2024. 2, 8
- [50] Lvmin Zhang, Anyi Rao, and Maneesh Agrawala. Adding conditional control to text-to-image diffusion models. In *ICCV*, pages 3836–3847, 2023. 2
- [51] Richard Zhang, Phillip Isola, Alexei A Efros, Eli Shechtman, and Oliver Wang. The unreasonable effectiveness of deep features as a perceptual metric. In *CVPR*, pages 586–595, 2018. 6



# Exploring Optimal Latent Trajectory for Zero-shot Image Editing

## Supplementary Material

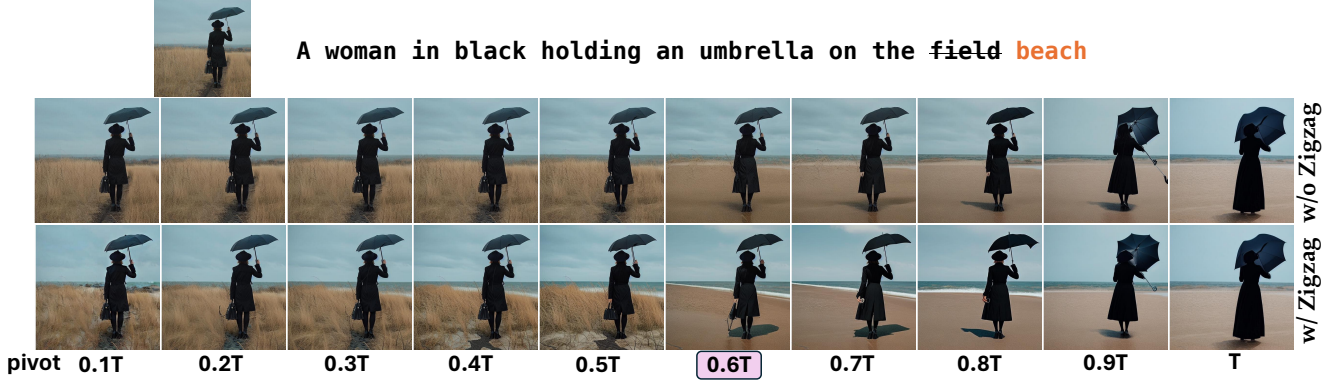


Figure 7. More ablation results of applying ZZEdit on P2P [15] w/ DDIM inversion, where different inverted latents are used with or without the ZigZag process equipped.

This supplementary material includes 4 sections. Sec. A gives more ablation study results. Sec. B provides more visualization in our ZZEdit using cross-attention maps. Sec. C illustrates more qualitative results to compare our results with state-of-the-art image editing methods. Sec. D introduces the limitations and future work of our ZZEdit.

### A. More Ablation Study

**Different Editing Pivot in ZZEdit.** We provide the visualization results using different points on the inversion trajectory as the editing pivot in Fig. 4 of our main paper. Here, we display one more visualization example of editing the background from 'field' to 'beach' in A-Fig. 7. We mark our located editing pivot with purple. Although the background corresponding to low-degree inversion is well maintained, its editability is insufficient. In contrast, a high-degree inversion brings editability but loses fidelity gradually. To better evaluate the effect of different editing pivots, as shown in A-Fig. 11 and A-Fig. 12, we leverage GPT-4V(ision) system [28], which gives the editing comments by a Multimodal LLMs.

**The Effectiveness and Distribution of Our Located Pivot.** In Tab. 1 of our main paper, we give the performance of selecting editing pivot from  $[0.1T, 0.2T, \dots, 0.9T, T]$  randomly based on the P2P [15] w/ DDIM inversion, where the standard ZigZag process ( $a = 1$ ) is equipped. In A-Tab. 3, we also report the corresponding performance using P2P w/ NTI [26] and PnP [43] w/ DDIM inversion. It delivers excellent background and structure preservation, but very poor editability. This also demonstrates the efficiency of our located pivot. Besides, as seen in A-Fig. 8, we provide the distribution of the editing pivots in our ZZEdit on the PIE-

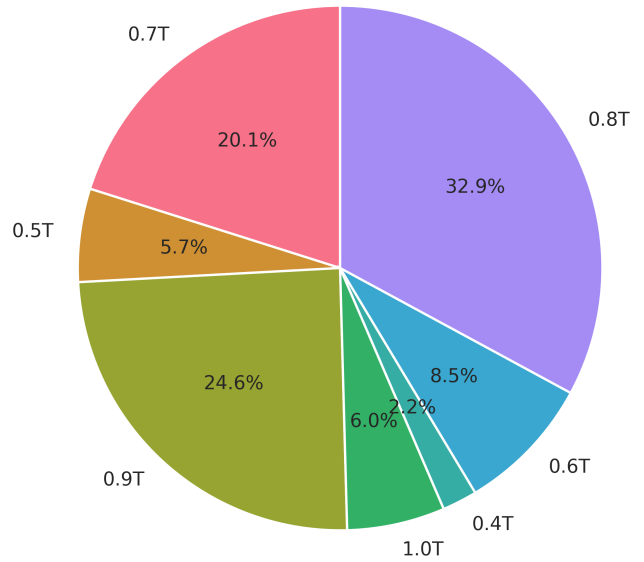


Figure 8. The statistics on the editing pivot located by our ZZEdit on the PIE-Bench dataset [19].

Bench dataset [19]. Note that to save time and computation, we only look for the pivot from  $[0.4T, 0.5T, \dots, 0.9T, T]$  in practice. When the pivot reaches  $T$  (i.e.,  $P = T$ ), our ZZEdit degenerates into the typical “inversion-then-editing” pipeline.

**The Effectiveness of The ZigZag Process.** As seen in A-Tab. 3, we additionally provide the corresponding quantitative ablation results using PnP w/ DDIM inversion and P2P w/ NTI. With the increase of  $a$ , our proposed Zigzag process gradually increases editing consistency, thus obtaining better CLIP similarity. While editing consistency increases,

Table 3. Quantitative ablation study on the proposed ZigZag process with PnP [43] w/ DDIM inversion and P2P [15] w/ Null-text inversion. Results are obtained on the PIE-Bench dataset [19]. The best results in the ZigZag process are marked in bold. Here, the results of random pivot with the ZigZag process are also provided.

Method		Structure	Background Preservation				CLIP Similarity	
		L2 ↓	PSNR ↑	LPIPS ↓	MSE ↓	SSIM ↑	Whole ↑	Edited ↑
<b>PnP+DDIM Baseline</b>		28.22	22.28	113.46	83.64	79.05	25.41	22.62
<i>w/ Pivot</i>	<i>w/o ZigZag (a = 0)</i>	<b>19.37</b>	<b>25.48</b>	<b>77.91</b>	<b>50.11</b>	<b>83.09</b>	24.94	22.22
	<i>w/ ZigZag (a = 0.2)</i>	20.06	25.29	79.94	50.99	82.91	25.00	22.33
	<i>w/ ZigZag (a = 0.6)</i>	21.94	24.86	84.69	54.01	82.41	25.11	22.54
	<i>w/ ZigZag (a = 1)</i>	23.46	24.55	86.10	55.04	82.18	<b>25.43</b>	<b>22.91</b>
<b>Random Pivot <i>w/ ZigZag (a = 1)</i></b>		12.53	27.16	66.57	35.43	83.91	24.16	21.30
<b>P2P+NTI Baseline</b>		13.44	27.03	60.67	35.86	84.11	24.75	21.86
<i>w/ Pivot</i>	<i>w/o ZigZag (a = 0)</i>	<b>4.97</b>	<b>29.79</b>	<b>36.62</b>	<b>19.89</b>	<b>86.71</b>	23.93	20.94
	<i>w/ ZigZag (a = 0.2)</i>	5.20	29.64	37.17	20.14	86.66	23.99	21.08
	<i>w/ ZigZag (a = 0.6)</i>	11.47	27.42	53.92	31.23	84.98	24.95	22.01
	<i>w/ ZigZag (a = 1)</i>	16.15	26.67	84.28	49.06	82.14	<b>25.16</b>	<b>22.13</b>
<b>Random Pivot <i>w/ ZigZag (a = 1)</i></b>		14.72	26.29	76.71	44.47	82.72	24.44	21.43

the performance of background preservation and structural information is slightly weakened.

## B. More Visualization of ZZEdit

We use cross-attention maps to reflect the response level of different-inverted latent  $z_t$  to the target prompt  $\mathcal{P}_{tgt}$ , where  $t \in [0.2T, 0.4T, 0.6T, 0.8T, T]$ . As shown in A-Fig. 9, a lot of intermediate-inverted latents can provide a considerable editability compared with fully-inverted  $z_T$ .

## C. More Image Editing Results

As shown in A-Fig. 10, we show more qualitative comparison with the current text-driven editing methods, including P2P [15] w/ DDIM inversion and w/ NTI, PnP [43] w/ DDIM inversion, Pix2Pix-Zero [29], MagicBrush [49], and Masactrl [6]. The editing scenario here includes *attribute editing*, *object replacement*, *style transfer and background editing*. Note that P2P w/ NTI often suffers from the color leak issue (see the 1-st and 5-th examples). The improvements are mostly tangible, and we circle some of the subtle discrepancies of the P2P and PnP baselines and the other compared methods in red.

## D. Limitations And Future Work

While our method achieves promising results, it still faces some limitations. First, our ZZEdit paradigm needs to find a suitable pivot before editing, which takes some time. Generally speaking, on a single Tesla A100 GPU, it takes about 23 seconds for an input image on average. Second, we mainly apply ZZEdit into P2P and PnP, where the baseline model cannot generate new motion (e.g., ‘standing’  $\rightarrow$  ‘fly’). Exploring optimal latent trajectory cannot endow these baseline models with motion-editing capacities.

We find that GPT-4V [28] can act as a good editing evaluator, so we hope to use it to build a new GPT-4V evaluation metric for text-driven image editing in the future. Besides, for further motion editing, we will leverage our ZZEdit paradigm on the generic pretrained diffusion model for motion editing abilities.

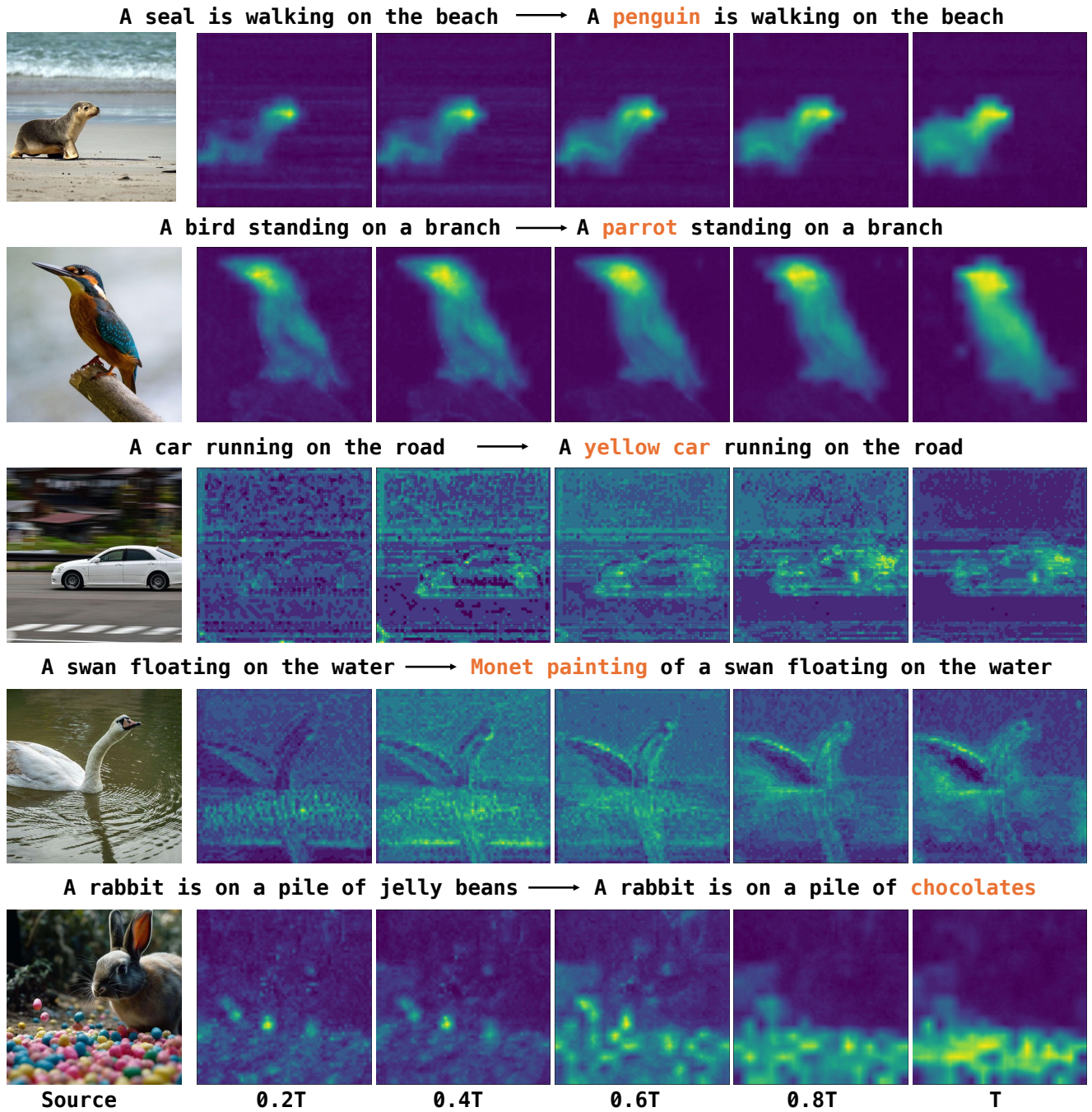


Figure 9. The cross-attention maps between different inverted latents  $z_t$  and the target prompt  $\mathcal{P}_{tgt}$ , where  $t \in [0.2T, 0.4T, 0.6T, 0.8T, T]$ .





Figure 10. More visualization results of different editing techniques.



: Given the image and the editing prompt, how to evaluate the following editing results?



### : Row 1 (Images 2-11)

- **Early Images (2-5):** These show subtle changes, primarily in color, without altering the bird's physical structure significantly. They do not yet achieve a distinct parrot appearance.
- **Middle Images (6-8):** Here, the changes become more pronounced, especially in terms of color and some slight alterations to the beak and tail. These images start to blend features of both a kingfisher and a parrot.
- **Later Images (9-11):** These images show more advanced transformations where the beak shape, color patterns, and overall morphology are more reminiscent of a parrot. Image 11, in particular, features a complete color transformation with a vivid red and green palette that is very characteristic of many parrot species.

### Row 2 (Images 12-21)

- **Early Images (12-14):** These continue to build on the transformation, experimenting with different color schemes that align more with various parrot species.
- **Middle Images (15-17):** These edits introduce more dramatic changes to the beak and head structure, aiming for a more realistic parrot look. Image 17 stands out with a well-defined parrot beak and a balanced color scheme that blends naturally.
- **Later Images (18-21):** These images might push the transformation a bit too far, as some edits introduce elements (like the green leaves or overly saturated colors) that detract from the realistic portrayal of a parrot.

### Conclusion

**Image 17** from Row 2 appears to be the best transformation. This image effectively balances the transition into a parrot by incorporating realistic alterations to the beak, head, and body while maintaining natural color blending and textural details. The image achieves a believable transformation from a kingfisher to a parrot, adhering closely to the editing prompt with high visual quality.

Figure 11. Using GPT-4V(ision) system [28] for evaluating the editing example of Fig. 4 in our main paper. Here, we explore the effect of using different inversion-degree latent as the editing pivot with or without the ZigZag process equipped. We suggest using Fig. 4 as a reference.



: Given the image and the editing prompt, how to evaluate the following editing results?



### : Row 1 (Images 2-11)

- **Images 2-5:** Gradual fading of the field into the beach. The earlier images retain more of the field, and by images 4 and 5, the beach starts to become more prominent.
- **Images 6-8:** These images show an effective blend where the beach setting becomes dominant. Image 8, in particular, stands out with a clear, well-integrated beach background that matches the lighting and perspective correctly.
- **Images 9-11:** Full transition to the beach is completed. Image 10 adjusts the position and angle slightly, which might affect the perceived naturalness of the setting.

### Row 2 (Images 12-21)

- **Images 12-14:** Initiation of the transition with subtle changes in the background. These are more tentative steps towards the beach setting.
- **Images 15-17:** Clear beach backgrounds are established here, with changes in the position and orientation of the woman to better suit the new setting. Image 17 is particularly notable for its realistic integration of the subject with the beach environment.
- **Images 18-21:** These final images explore different angles and further adjustments to the background and the subject's placement. Image 20 offers a dynamic angle with a strong visual composition that aligns well with the beach environment.

### Conclusion

**Image 17** from Row 2 is the best transformation among all 20 images. This image showcases a fully realized beach setting with a natural and convincing placement of the woman. It achieves a seamless integration by matching the lighting conditions and perspective, ensuring the subject fits organically into the beach environment. The composition is harmonious, and the transition from the original field setting is handled smoothly, making it a standout in fulfilling the editing prompt effectively.

Figure 12. Using GPT-4V(ision) system [28] for evaluating the editing example of A-Fig. 7 in this supplement. Here, we explore the effect of using different inversion-degree latent as the editing pivot with or without the ZigZag process equipped. We suggest using A-Fig. 7 as reference.